Effect of Waveform Parameters on Pulsed Glow Discharge in Air

Fengbo Tao[1], Zhicheng Zhou[1], Yong Ma[1], Qiaogen Zhang[2]

[1]Jiangsu Electric Power Research Institute, Nanjing, China
[2]School of Electrical Engineering, Xi'an Jiaotong University, Xi'an, China
Email: hvtaofb@gmail.com

ABSTRACT

The nanosecond single pulse was employed here to generate a large volume glow discharge between the wire-plane electrodes in air. In order to find requirements on pulse waveform for generation of a large volume discharge at atmospheric pressure, the effect of pulse risetime, pulse width, and amplitude on glow discharge has been widely investigated in this paper. Results reveal that a large volume glow discharge can be generated in an inhomogeneous electric field under the single pulse with the faster risetime, the lower peak amplitude. The pulse width has almost no influence on the density of glow discharge, but which has a great influence on the transition from glow discharge to streamer discharge. A model of inter-shielding-effect has been proposed to explain the influence of waveform parameters on pulsed glow discharge.

Keywords: Pulsed Discharge; Large Volume Glow Discharge; Inter-Shielding-Effect

1. Introduction

Gas plasma generated by pulse discharge is widely used in ozone generation [1-3], detoxification of gaseous pollution [4-6], material surface treatment [7,8], synthesis of nanostructured material [9,10], etc. In order to improve the efficiency of the applications mentioned above, the homogeneous, large volume discharge is required. From the previous works, it can be seen that nanosecond pulse discharge in non-uniform electric field constructed by needles-plane or wire-plane electrodes is an efficient way to obtain large volume discharge. For instance, Ryo Ono and Tetsuji Oda have used the pulsed discharge between needles-plane electrodes to generate ozone and measured the ozone distribution in the discharge gap. R. A. Roush and R. K. Hutcherson focused on the exhaust gas detoxification efficiency by large volume discharge under different pulse risetime and pulse width [11-13]. Although the large volume discharge is widely used in the industry applications, the effect of waveform parameters on the formation of large volume discharge is not very clear yet. In order to find requirements on pulse waveform for generation of a large volume discharge at atmospheric pressure and understand more clearly the mechanism of pulsed discharge, a single pulse voltage with adjustable risetime, pulse width, amplitude etc is employed here to investigate the formation of the large volume discharge between the wire-plane electrodes with non-uniform electric field.

2. Experimental Set-Up

Figure 1 shows the schematic experimental circuit employed in this research. A single pulse with the pulse risetime from 10 ns to 500 ns, pulse width from 100 ns to 2 µs, peak amplitude from 10 kV to 50 kV was applied on the wire-plane electrodes. A rogowski brass plane of 60 mm in diameter was used as the cathode, and a brass wire of 0.1 mm in diameter was used as the anode. Also, the wire of 100 mm in length, longer than the diameter of the cathode, was used to prevent the edge effect of the two electrodes. The gap distance was fixed at 8mm. Both electrodes were sealed in a polymethyl methacrylate container. The air pressure in the chamber can be adjusted in the range of 2 kPa to 0.2 MPa.

The pulse voltage was measured with the voltage divider consisting of (R_1 & C_1) and (R_2 & C_2), which has the response time less than 5 ns. The discharge current was measured with a current transducer (rogowski coil), which has the response time less than 5 ns. The voltage and current signals were recorded by a digitizing oscilloscope (Tektronix DPO4054) with a bandwidth of 500 MHz. Considering that the discharge images are in correspondence with one-off discharge process caused by the nanosecond single pulse, there will be no superposition of repetitious discharges, so the exposure time is
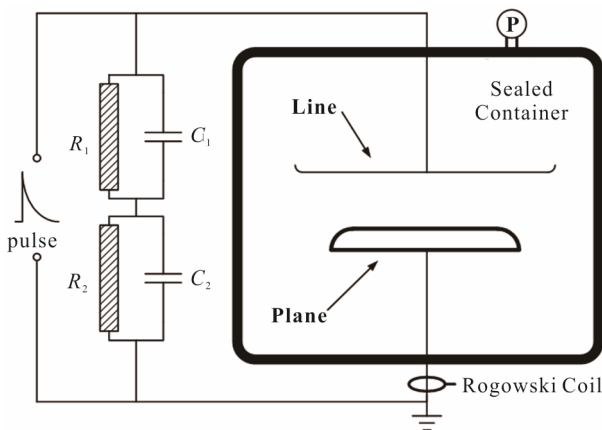
Figure 1. Schematic diagram of the electrode system and the experimental set-up.
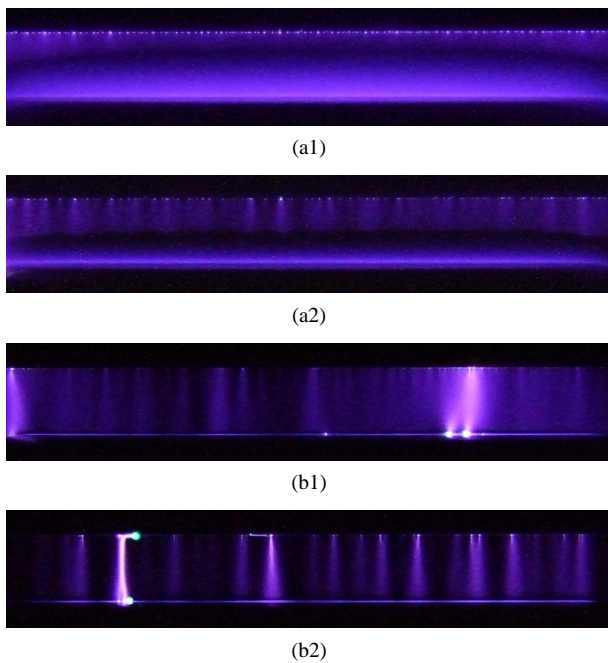

(a1)

(a2)

(b1)

(b2)

Figure 2. Pulsed discharge images with different pulse risetimes at different air pressures ((a1) 20 ns/6 kPa; (a2) 200 ns/6 kPa; (b1) 20 ns/15 kPa; (b2) 200 ns/15 kPa).

determined by the pulsed discharge time. Furthermore, due to the high resolution and the high sensitivity of the ordinary camera, detail of the discharge channel can be observed more clearly. Therefore, the images of the discharges were captured by a camera (FUJIFILM FinePix S6500) with a resolution of 2848 × 2136 pixels in a single shot with the exposure time of (1/3) s.

3. Experimental Results and Discussions

3.1. Effect of Pulse Risetime

Figure 2 shows the images of pulsed glow discharge in wire-plane air gap with the pulse risetime of 20 ns and
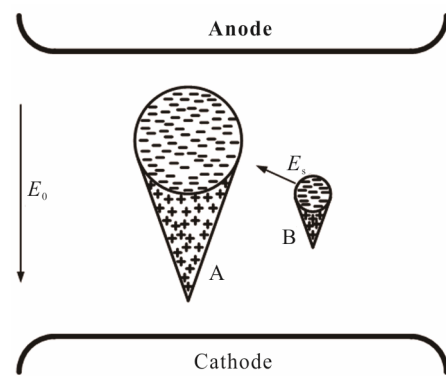

Figure 3. Schematic diagram of inter-shielding-effect between avalanches.

200 ns respectively. The pulse width and peak amplitude are fixed at 200 ns and 20 kV respectively. Experiments were carried out at the air pressure of 6 kPa and 15 kPa. For all images in this paper, the upper is wire anode electrode and the opposite is plane ground electrode.

From **Figure 2**, it can be seen that at the same gas pressure, in the case of fast pulse with risetime of 20 ns, the white spots called spot glow by Anatoly Nikolaevich Maltsev near anode [14], are much more in number than those in the case of the slow pulse with risetime of 200 ns. This can be explained by the inter-shielding-effect. Because of the different delay times in the formation of the primary electrons around the anode, some avalanches grow ahead and distort the electric field in the gap, which leads to the suppressing of the adjacent avalanches. The schematic diagram of inter-shielding-effect is illustrated in **Figure 3**, in which E_0 is the applied electric field, A is the preceding avalanche, and B is the posterior avalanche, E_S is the space charge electric field formed by A around the head of the posterior avalanche B. When E_S is large enough to cause the total electric field unsatisfied for the development of B, the growth of the posterior avalanche B will stop.

Assuming that there is the delay time (τ_0) of the primary electron formation. Avalanche A grows ahead of avalanche B at the time of τ_0 early. The growth of avalanche A results in accumulation of the space charges in the head of avalanche A as well as the decrease of electric field E_S around the head of the posterior avalanche B, which leads to the suppressing of avalanche B and the decrease of white spots around the anode. The following expression can also clarify the effect of pulse risetime on glow discharge [15].

$$\frac{1}{2}n\mu\left(\frac{E}{n}\right)_0 t_0 < r_c, \quad r_c = \left(40\xi_c/nQ\right)^{1/2} \tag{1}$$

where, t_0 is the pulse risetime when applied E/n has reached $(E/n)_0$, r_c is critical radius of avalanche head, μ is the electron mobility, ξ_c is critical length of avalanche, Q

is the averaged momentum transfer cross section. From expression (1), we can see that with the decrease of pulse risetime, expression (1) can be quite easily satisfied, *i.e.* the overlapping condition between electron avalanches can be fulfilled. Furthermore, with the increase of air pressure, the risetime of pulse is required to decrease further to fulfill expression (1).

3.2. Effect of Pulse Amplitude

Figure 4 shows the images of the pulsed glow discharge under the pulse amplitude of 20 kV and 35 kV respectively. The experiments were carried out at different gas pressures: 20 kPa, 40 kPa and 60 kPa. The pulse risetime and pulse width are fixed at 20 ns and 120 ns respectively.

In **Figure 4**, the number of discrete channels in pulsed glow discharge decreases with the increase of peak amplitude. Moreover, the discrete channels can easily come

into streamer discharge (the white channels illustrated in **Figures 4(a2)-(c2)** in the case of higher pulse amplitude due to the current heat effect. As mentioned above, the early or late growth of avalanches will form the uneven distribution of the current in each discrete channel. With the increase of the pulse amplitude, the higher overvoltage promotes the growth of avalanche A as well as the formation of space charge electric field (E_S), which results in the further increase of inter-shielding-effect on avalanche B. Therefore, the increase of pulse amplitude will cause the decrease of the discrete channel number as well as the increase of current in each channel. Due to the uneven distribution and the increase of the current in discrete channels, the early propagated channel will transit into streamer or spark discharge, which results in the current and the luminescence decrease in other discrete channels, as shown in **Figures 4(a2)-(c2)**.

The discharge current waveforms with different pulse amplitude at the air pressure of 20 kPa are illustrated in **Figures 5(a)** and **(b)**. It can be found that there are some fluctuations on the current waveforms, which are related to the formation of avalanches during the discharge process. Due to the greater inhibition between avalanches at high pulse amplitude, the number of fluctuations on the current waveform under 35 kV pulse (**Figure 5(b)**) is

(a1)
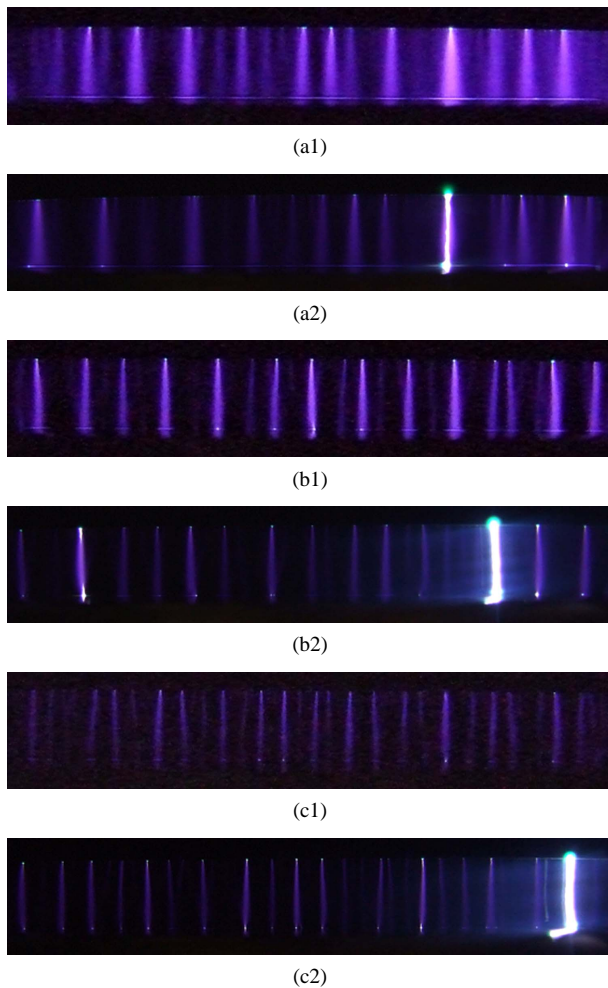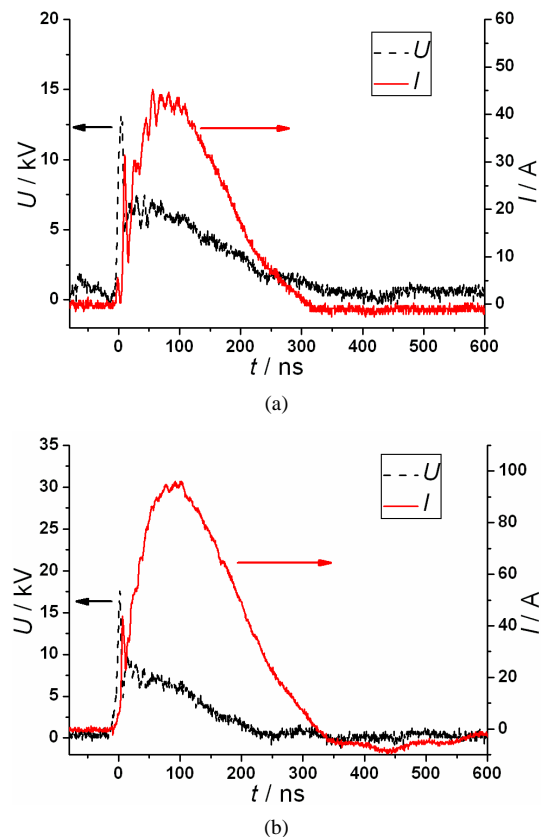
(a2)

(b1)

(b2)

(c1)

(c2)

Figure 4. Pulse discharge images with different pulse peak amplitude at different air pressure ((a1) 20 kPa/20 kV; (a2) 20 kPa/35 kV; (b1) 40 kPa/20 kV; (b2) 40 kPa/35 kV; (c1) 60 kPa/20 kV; (c2) 60 kPa/35 kV).

(a)

(b)

Figure 5. Current waveforms of pulse discharge under different amplitude in 20 kPa. (a) U_p = 20 kV; (b) U_p = 35 kV.

less than that under 20 kV pulse (**Figure 5(a)**).

From **Figure 5**, It can also be found that due to the streamer discharge, the peak discharge current under 35 kV pulse is larger than that under 20 kV pulse, the voltage collapse time under 35 kV pulse is less than that under 20 kV pulse. A slight oscillation on the tail of the current waveform under the pulse amplitude of 35 kV can also be seen, which is caused by the streamer discharge illustrated in **Figure 4**.

3.3. Effect of Pulse Width

Effect of the pulse width on the pulsed glow discharge is investigated by varying the pulse width from 120 ns to 1600 ns at the air pressure of 40 kPa. **Figure 6** illustrates the images of large volume discharges under different pulse width with the fixed pulse risetime of 20 ns and peak amplitude of 20 kV.

From **Figure 6**, it can be clarified that the pulse width in the range from 120 ns to 1600 ns has little influence on the number and luminescence of the discrete channels in the pulsed glow discharge, but the increase of the pulse width will cause the transition from glow discharge to streamer or spark discharge easily. As discussed in part A, the discharge mode in the gap applied by pulsed voltage is dominated by the pulse risetime. Therefore, for a given pulse risetime, the number of the discrete channels is basically invariable and is not affected by the pulse width as shown in **Figure 6**. However, when increasing the pulse width, the higher energy will be injected into the discharge channel, which results in the
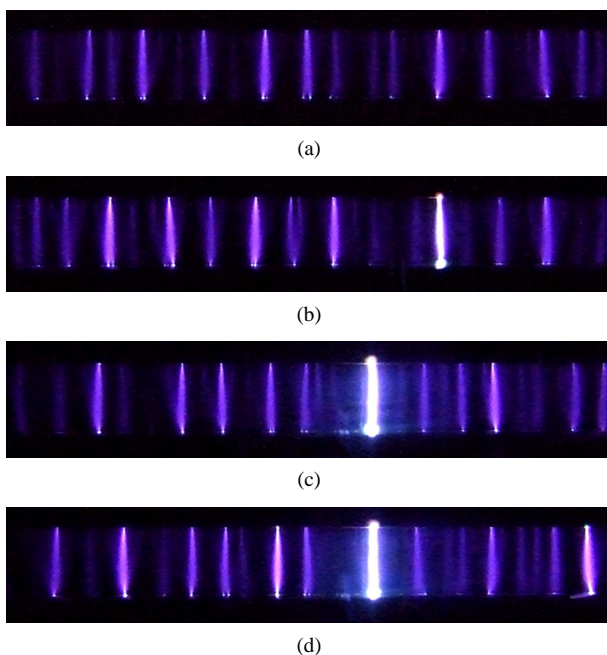
transition from glow discharge to streamer or spark discharge in the early propagated channel due to the uneven distribution of the current. In **Figure 6**, the luminescence of the other discrete channels is nearly not influenced by the pulse risetime, which can be considered that the increased pulse energy is almost injected into the early propagated channel with the increase of pulse width.

The discharge current waveforms under different pulse width are illustrated in **Figure 7**, the part in the range of 0 - 150 ns is zoomed at the top right corner. From **Figure 7**, it can be seen that at the first 60 ns, the pulse discharge current waveforms for different pulse width are almost the same, which is controlled by the growth of the pulsed glow discharge channels as shown in **Figure 6**, *i.e.* the number of the discrete channels as well as its distribution is determined by the pulse risetime. After the pulse reaches the peak value, the discharge development is determined by the pulse width. With the increase of the pulse width, the increased energy is injected into the early propagated channel, resulting in the increasing of the discharge current including the increase of the luminescence in the early propagated channel.

4. Conclusion

In this paper, pulsed glow discharge is generated in air between wire and plane electrodes with non-uniform electric field. The effect of pulse risetime, pulse width and amplitude on glow discharge has been widely investigated. Results reveal that a large volume glow discharge can be generated in an inhomogeneous electric field more easily under the pulse with faster risetime. The pulse width has almost no influence on the mode of glow discharge, but has a great influence on the transition from glow discharge to streamer discharge. A model of inter-shielding-effect has been proposed to explain the
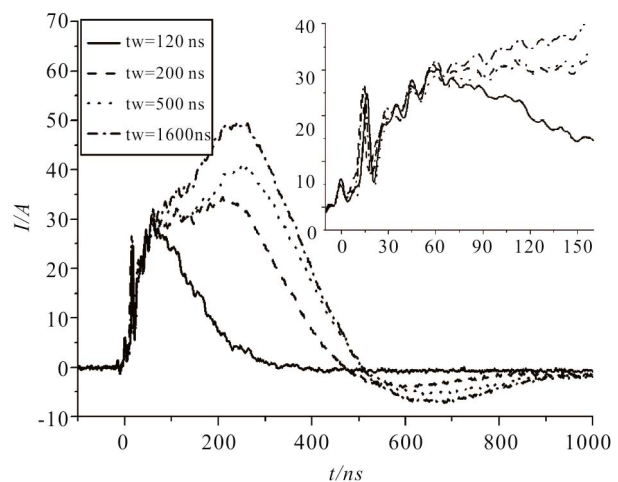

(a)

(b)

(c)

(d)

Figure 6. Images of pulse discharge with different pulse width (a) 120 ns; (b) 200 ns; (c) 500 ns; (d) 1600 ns.

Figure 7. Pulse discharge current under different pulse width.

influence of waveform parameters on the pulsed glow discharge.

REFERENCES

[1] W. Samaranayake, Y. Miyahara, T. Namihira, *et al.*, "Ozone Generation in Dry Air Using Pulsed Discharges with and without a Solid Dielectric Layer," *IEEE Transactions on Dielectrics and Electrical Insulation*, Vol. 8, No. 4, 2001, pp. 687-697. [doi:10.1109/94.946724](doi:10.1109/94.946724)

[2] R. Ono and T. Oda, "Ozone Production Process in Pulsed Positive Dielectric Barrier Discharge," *Journal of Physics D*: *Applied Physics*, Vol. 40, No. 1, 2007, pp. 176-182. [doi:10.1088/0022-3727/40/1/011](doi:10.1088/0022-3727/40/1/011)

[3] M. Simek and M. Clupek, "Efficiency of Ozone Production by Pulsed Positive Corona Discharge in Synthetic Air," *Journal of Physics D*: *Applied Physics*, Vol. 35, No. 11, 2002, pp. 1171-1175. [doi:10.1088/0022-3727/35/11/311](doi:10.1088/0022-3727/35/11/311)

[4] Y. Yankelevich and A. Pokryvailo, "High-Power Short-Pulsed Corona: Investigation of Electrical Performance, SO_2 Removal, and Ozone Gene*ration*," *IEEE Transactions on Plasma Science*, Vol. 30, No. 5, 2002, pp. 1975-1981. [doi:10.1109/TPS.2002.805320](doi:10.1109/TPS.2002.805320)

[5] F. Fresnet, G. Baravian, L. Magne, *et al.*, "Influence of Water on NO Removal by Pulsed Discharge in $N_2/H_2O/$ NO Mixtures," *Plasma Source Science and Technology*, Vol. 11, No. 2, 2002, pp. 152-160. [doi:10.1088/0963-0252/11/2/305](doi:10.1088/0963-0252/11/2/305)

[6] T. Namihira, S. Tsukamoto, D. Wang, *et al.*, "Influence of Gas Flow Rate and Reactor Length on NO Removal Using Pulsed Power," *IEEE Transactions on Plasma Science*, Vol. 29, No. 4, 2001, pp. 592-598. [doi:10.1109/27.940952](doi:10.1109/27.940952)

[7] T. Yuji and Y. Sung, "Surface Treatment of TiO_2 Films by Pulse Plasma for Dye-Sensitized Solar Cells Application," *IEEE Transactions on Plasma Science*, Vol. 35, No. 4, 2007, pp. 1010-1013. [doi:10.1109/TPS.2007.896918](doi:10.1109/TPS.2007.896918)

[8] N. Takeuchi, K. Yasuoka and S. Ishii, "Surface Modification of Thin Rods by Theta-Pinching Metallic Plasmas," *IEEE Transactions on Plasma Science*, Vol. 34, No. 4, 2006, pp. 1112-1115. [doi:10.1109/TPS.2006.876484](doi:10.1109/TPS.2006.876484)

[9] W. D. Yang, P. N. Wang, F. M. Li and K. W. Cheah, "Synthesis of Oxygen-Free Nanosized InN by Pulse Discharge," *Nanotechnology*, Vol. 13, No. 1, 2002, pp. 65-68. [doi:10.1088/0957-4484/13/1/315](doi:10.1088/0957-4484/13/1/315)

[10] H. Yang, W. Nam and D. Park, "Production of Nanosized Carbon Black from Hydrocarbon by a Thermal Plasma," *Journal of Nanoscience and Nanotechnology*, Vol. 7, No. 11, 2007, pp. 3744-3749. [doi:10.1166/jnn.2007.003](doi:10.1166/jnn.2007.003)

[11] R. Ono and T. Oda, "Dynamics of Ozone and OH Radicals Generated by Pulsed Corona Discharge in Humid-Air Flow Reactor Measured by Laser Spectroscopy," *Journal of Applied Physics*, Vol. 93, No. 10, 2003, pp. 5876-5882. [doi:10.1063/1.1567796](doi:10.1063/1.1567796)

[12] R. Roush, R. Hutcherson, M. Ingram, *et al.*, "Effects of Pulse Risetime and Pulse Width on the Destruction of Toluene and NO_X in a Coaxial Pulsed Corona Reactor," *Proceeding of* 22*nd IEEE International Power Modulator Symposium*, Boca Raton, 25-27 June 1996, pp. 79-84.

[13] D. Wang, M. Jikuya, S. Yoshida, *et al.*, "Positive- and Negative-Pulsed Streamer Discharges Generated by a 100-ns Pulsed-Power in Atmospheric Air," *IEEE Transacitions on Plasma Science*, Vol. 35, No. 4, 2007, pp. 1098-1103. [doi:10.1109/TPS.2007.902132](doi:10.1109/TPS.2007.902132)

[14] A. N. Maltsev, "Dense Gas Discharge with Runaway Electrons as a New Plasma Source for Surface Modification and Treatment," *IEEE Transactions on Plasma Science*, Vol. 34, No. 4, 2006, pp. 1166-1174. [doi:10.1109/TPS.2006.878994](doi:10.1109/TPS.2006.878994)

[15] J. I. Levatter and S.-C. Lin, "Necessary Conditions for the Homogeneous Formation of Pulsed Avalanche Discharge at High Gas Pressure," *Journal of Applied Physics*, Vol. 51, No. 1, 1980, pp. 210-222. [doi:10.1063/1.327412](doi:10.1063/1.327412)